AJNR

Asymmetric appearance of intracranial vessels on routine spin-echo MR images: a pulse sequence-dependent phenomenon.

N Fujita, K Harada, N Hirabuki, K Fujii, Y Akai, T Hashimoto, T Miura, M Mitomo and T Kozuka

AJNR Am J Neuroradiol 1992, 13 (4) 1153-1159
http://www.ajnr.org/content/13/4/1153

Asymmetric Appearance of Intracranial Vessels on Routine Spin-Echo MR Images: A Pulse Sequence-Dependent Phenomenon

Norihiko Fujita,[1] Koushi Harada,[1] Norio Hirabuki,[1] Keiko Fujii,[1] Yoshinori Akai,[1] Tsutomu Hashimoto,[1] Takashi Miura,[1] Masanori Mitomo,[1] and Takahiro Kozuka[1]

Purpose: To determine the cause of right to left signal intensity differences arising from intracranial vessels during routine spin-echo axial MR imaging of the head. **Methods and Results:** Using a normal imaging sequence in which the default directions of the frequency and phase axes were horizontal and vertical, respectively, differences in signal intensity arising from the vertebral arteries were observed in a healthy subject. With the exchange of the frequency and phase axes relative to the normal sequence, no signal intensity differences between the vertebral arteries were recognized. Other pulse sequence modifications, ie, the use of motion-compensating gradients and the reversed polarity of the frequency-encoding gradient, also resulted in variable appearances of the vertebral arteries, indicating that the right-to-left signal asymmetry of the vertebral arteries observed on the normal spin-echo image results from a pulse sequence dependent phenomenon. **Conclusions:** Frequency-encoding and slice-selection gradients both produce motion-induced phase shifts. These phase shifts depend on the angle between the direction of flow and that of the effective vector sum of these gradients. The asymmetric appearance of the vertebral arteries during normal spin-echo imaging was found to result from the angle dependence of motion-induced phase shifts. Awareness of this artifactual phenomenon is important to avoid confusing it with conditions such as stenosis/occlusion, dissection, or slow flow.

Index terms: Magnetic resonance, artifacts; Arteries, vertebral

AJNR 13:1153–1159, Jul/Aug 1992

A pair of right and left intracranial vessels imaged with any magnetic resonance (MR) pulse sequence, when symmetrically positioned in an axial or coronal section, are expected to have identical signal intensities. Conversely, when intraluminal signal intensity differences between right and left intracranial vessels are seen, the presence of abnormalities such as stenosis/occlusion, dissection, or slow flow is suspected on one side (1–5).

During routine head examinations of patients at our institution on a 1.5-T MR unit (Magnetom, Siemens AG, Erlangen, Germany), we often noticed right-to-left asymmetry in signal intensity arising from intracranial vessels. In particular, signal intensity differences between a pair of vertebral arteries were often seen and were always represented on T1-weighted spin-echo axial images as high intensity on the right side and iso to low intensity on the left. Initially, it was thought that this signal asymmetry might be ascribed to differences in flow characteristics between the right and left vertebral arteries. However, by chance, exchange of the frequency- and phase-encoding axes resulted in the disappearance of this signal asymmetry, with high intensity visible on both sides.

To better understand this phenomenon, we explored the origin of the right-to-left signal asymmetry in an asymptomatic subject by employing pulse sequence modifications such as reversed polarity of the imaging gradient, exchange of the frequency- and phase-encoding axes, and the use of motion-compensating gradients (6).

Received June 11, 1991; accepted and revisions requested August 21; revisions received October 18.

[1] All authors: Department of Radiology, Osaka University Medical School 1-1-50, Fukushima, Fukushima-ku, Osaka 553, Japan. Address reprint requests to Norihiko Fujita, MD.

AJNR 13:1153–1159, Jul/Aug 1992 0195-6108/92/1304-1153

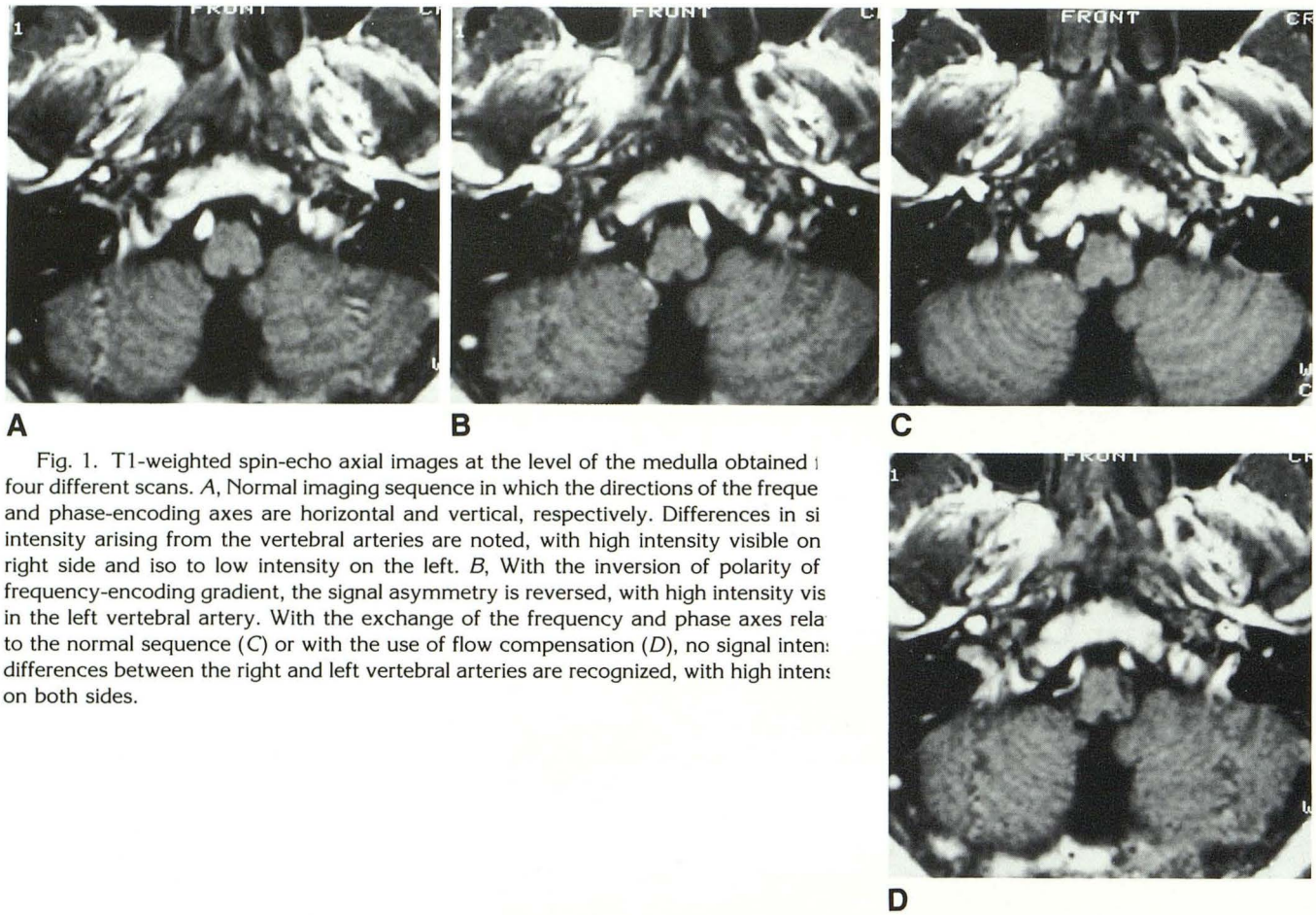

Fig. 1. T1-weighted spin-echo axial images at the level of the medulla obtained i four different scans. *A*, Normal imaging sequence in which the directions of the freque and phase-encoding axes are horizontal and vertical, respectively. Differences in si intensity arising from the vertebral arteries are noted, with high intensity visible on right side and iso to low intensity on the left. *B*, With the inversion of polarity of frequency-encoding gradient, the signal asymmetry is reversed, with high intensity vis in the left vertebral artery. With the exchange of the frequency and phase axes rela to the normal sequence (*C*) or with the use of flow compensation (*D*), no signal inten differences between the right and left vertebral arteries are recognized, with high inten on both sides.

Materials and Methods

Four sets of T1-weighted spin-echo axial images of the posterior fossa were obtained from an asymptomatic subject using a 1.5-T MR unit (Magnetom, Siemens AG). The imaging parameters were the same for the four sets: 500/15/2 (TR/TE/excitations), 256 × 256 matrix, 21-cm field of view, and 5-mm slice thickness with a 1-mm interslice gap. Consecutive multislice excitations were employed from the cephalad to the caudal direction. This corresponded to the default order of section excitation on the MR unit when an interslice gap was set.

The first scan was obtained using a T1-weighted spin-echo pulse sequence, which is routinely used in our institute. On the routine axial head examinations, the default directions of the frequency- and phase-encoding axes were horizontal and vertical, respectively. A second scan was obtained that was identical to the first one, with the exception that the polarity of the frequency-encoding gradient was reversed. For the third scan, the directions of the frequency- and phase-encoding axes were exchanged relative to the first scan. The fourth scan was performed using a spin-echo sequence with first-order gradient moment nulling (GMN) in the frequency-encoding and slice-selection directions. To achieve the same TE as other sequences, a higher sampling rate was employed, together with increased frequency-encoding gradient strength.

In addition to the T1-weighted spin-echo images, dual-echo axial spin-echo images, 2500/15-90/1, were also obtained. The standard gradient waveform without GMN, which was identical to that for the T1-weighted spin-echo sequence, was used for the first echo. For the second echo, first- and second-order GMN was employed in the frequency-encoding and slice-selection directions. The other imaging parameters were the same as described above. We finally obtained thin-slice (3 mm), sequential axial images using a spoiled gradient-echo sequence that was first-order flow compensated in the frequency-encoding and slice-selection directions. The imaging parameters were: 80/7/90° (TR/TE/flip angle), 192 × 256 matrix, and 21-cm field of view. Projection MR angiograms were also created from the stack of the 2-D gradient-echo images by the use of a maximum-intensity projection algorithm.

Results

Figure 1 shows the T1-weighted spin-echo axial images at the level of the medulla obtained from the four different scans. On routine MR examinations of the head, the level of this section corresponds to the most caudal section or the subsequent few sections. The multislice excitation was done in a direction that is opposite to

the direction of inflowing arterial blood within the vertebral arteries. This would enable flow-related enhancement on several of the most inferior sections (7).

As shown in Figure 1A, corresponding to the routine spin-echo imaging, differences in signal intensity arising from the vertebral arteries are noted, with high intensity visible on the right side and iso to low intensity on the left. In Figure 1B, the signal asymmetry was reversed with the inversion of polarity of the frequency-encoding gradient. With the exchange of directions of the frequency- and phase-encoding axes (Fig. 1C) or with the use of motion-compensating gradients (Fig. 1D), no signal intensity differences arising from the vertebral arteries were visible, with high intensity on both sides.

Figure 2 shows the proton density-weighted, T2-weighted, and gradient-echo axial images at the corresponding level to Figure 1. The proton density-weighted image (Fig. 2A) demonstrated the asymmetric appearance of the vertebral arteries in the same way as seen in Figure 1A. The right and left vertebral arteries were symmetrically represented as low intensity on the T2-weighted image (Fig. 2B) and high intensity on the flow compensated gradient-echo image (Fig. 2C). The projection MR angiogram (Fig. 2D) demonstrated the symmetric appearance of the vertebrobasilar system.

Discussion

All flow phenomena in MR imaging are, in principle, explained by two basic properties (8–11): Time-of-flight effects, which simply relate to the change in position of spins during the imaging sequence, and phase-shift effects acquired by spins during motion occurring in the presence of magnetic field gradients. However, the signal intensity of flowing blood is affected in complicated ways that depend both on the details of the particular imaging technique employed and on the flow characteristics, including the direction of blood flow relative to the imaging plane. Blood flow phenomena occurring when flow is within the imaging plane, ie, in-plane flow phenomena, are predominantly due to spin-phase shifts re-

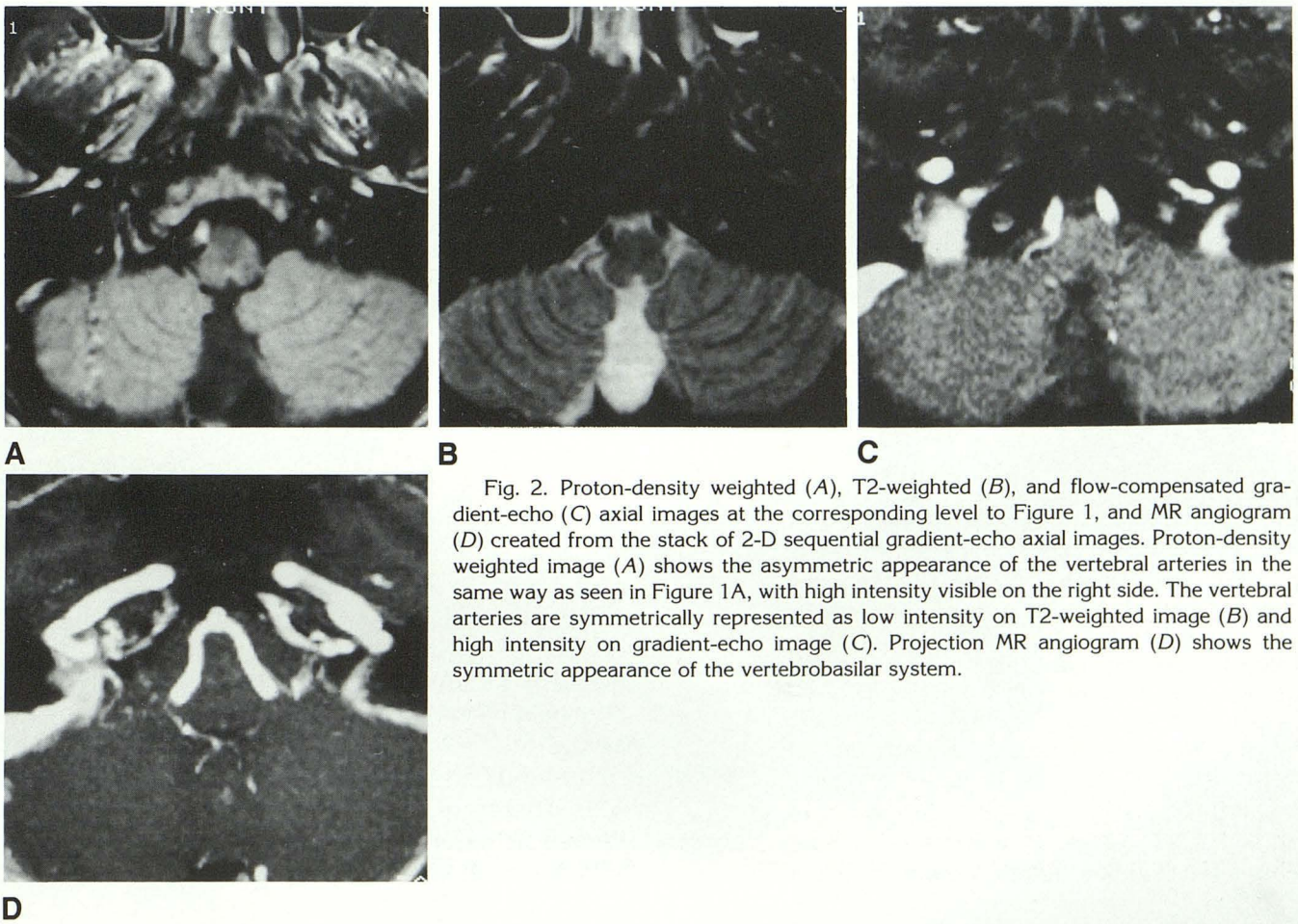

Fig. 2. Proton-density weighted (*A*), T2-weighted (*B*), and flow-compensated gradient-echo (*C*) axial images at the corresponding level to Figure 1, and MR angiogram (*D*) created from the stack of 2-D sequential gradient-echo axial images. Proton-density weighted image (*A*) shows the asymmetric appearance of the vertebral arteries in the same way as seen in Figure 1A, with high intensity visible on the right side. The vertebral arteries are symmetrically represented as low intensity on T2-weighted image (*B*) and high intensity on gradient-echo image (*C*). Projection MR angiogram (*D*) shows the symmetric appearance of the vertebrobasilar system.

sulting from motion in the frequency-encoding axis, and to a lesser extent from motion in the phase-encoding axis (11). A kind of time-of-flight effect, spatial misregistration of in-plane vascular flow, is caused by motion of spins during the time delay between the applications of the phase- and frequency-encoding gradients (11, 12). Blood flow phenomena occurring when flow is perpendicular to the imaging plane, ie, through-plane flow phenomena, are primarily dependent on time-of-flight effects, such as inflow signal enhancement and outflow signal loss (9, 10). At high velocities, spin-phase shifts, caused by motion in the slice-selection axis, play an additional role in the signal loss of flowing blood.

When the vessel traverses obliquely through the imaging plane, as shown in Figure 3, compounded effects of the in-plane and through-plane flow phenomena occur. As for time-of-flight effects, inflow signal enhancement and outflow signal loss contribute to the appearance of obliquely flowing spins, depending both on the slice-selection directional component of their velocities and on the particular imaging technique employed. A kind of time-of-flight effect, downstream mismapped signal of obliquely flowing spins, is caused by the time delay between the preceding radio frequency pulse experienced by slice-selected flowing spins and the subsequent readout (8, 12). With regard to motion-induced phase-shift effects, we must take into consideration spin-phase shifts resulting both from motion in the slice-selection direction and from motion in the imaging plane, ie, motion in the frequency- and phase-encoding directions (13). Since the contribution from motion in the phase-encoding direction is small compared to that from motion in the other directions, in the following discussion, we disregard the effects of motion-induced phase shifts in the phase-encoding direction (13) (see also Appendix).

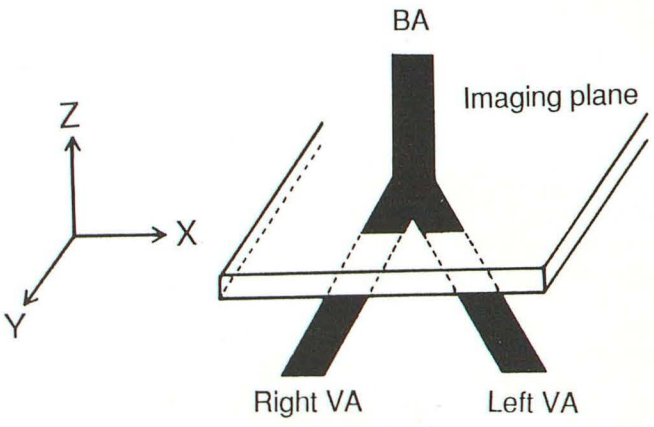

Fig. 3. Schematic representation of obliquely traversing vertebral arteries (*dotted line*) through axial imaging plane; *VA* = vertebral artery; *BA* = basilar artery. The default allocation of the imaging axes on the Siemens MR unit in axial imaging of the head is as follows: *X*-frequency, *Y*-phase, and *Z*-slice.

Slice-selection and frequency-encoding gradients are usually balanced gradients, which for stationary spins do not result in net phase shift during the sequence. However, these gradients both produce phase shifts for flowing spins. The motion-induced phase shifts depend on the angle between the direction of flow and that of the "gradient factor", ie, the effective gradient that flow experiences due to the combined effects of the slice-selection and frequency-encoding gradients (13) (see also Appendix).

Figure 4 illustrates the relationship between the flow directions in the vertebral arteries (*VA*s) and gradient factor projected in the plane determined by the slice-selection and frequency-encoding axes. With the help of Figure 4, we can explain the cause of the variable appearance of the *VA*s seen in Figure 1. Figure 4A corresponds to the first scan imaged (Fig. 1A) with the routinely used single spin-echo pulse sequence under the default setting of the horizontal frequency- and vertical phase-encoding directions. As shown in Figure 4A, the direction of GF had a nearly perpendicular orientation in relation to the orientation of flow in the right *VA*. Since no phase shifts occur when flow is perpendicular to the direction of a gradient, the accumulated phase due to motion in the right *VA* is minimal compared to that in the left *VA*. Due to the insensitivity to motion-induced phase-shift effects of the right *VA*, inflow signal enhancement becomes dominant, thereby leading to its high intensity seen in Figure 1A. For the left *VA*, the orientation is nearly parallel to the gradient factor, leading to maximal phase shifts because of motion. Therefore, the pulsatile nature of arterial flow would lead to varying phase shifts, resulting in a misregistration in the phase-encoding axis, and, hence, the subsequent signal loss of the left *VA* as seen in Figure 1A.

The inversion of polarity of the frequency-encoding gradient results in a rotation of the gradient factor about the slice-selection axis as shown in Figure 4B. In this case, the flow direction in the left *VA* is insensitive to motion-induced phase-shift effects compared to that in the right *VA*. Therefore, the signal asymmetry was reversed as seen in Figure 1B, with high intensity visible on the left. With the exchange of directions

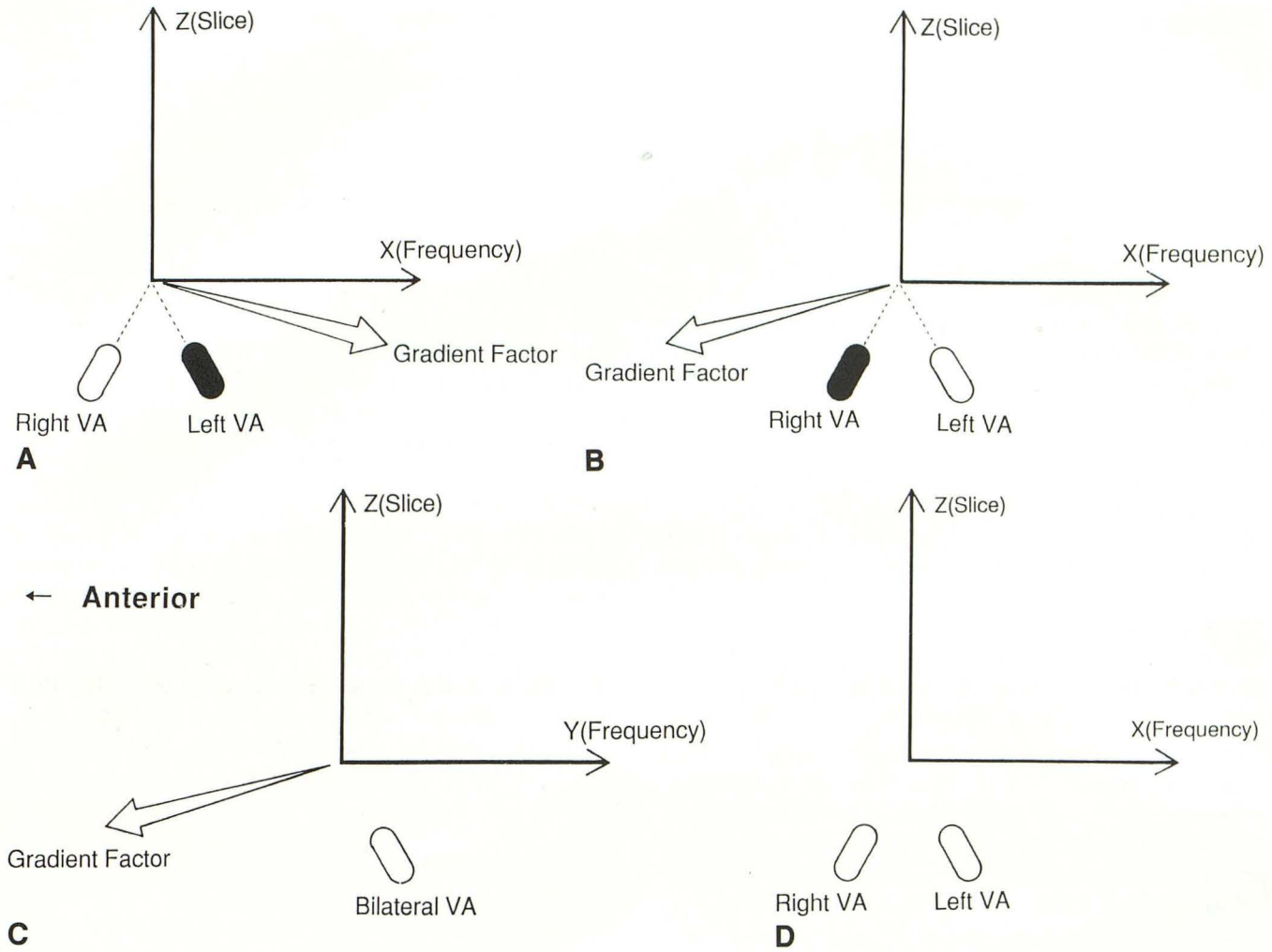

Fig. 4. Relationship between flow directions in the vertebral arteries (*VA*s) and gradient factors concerning motion-induced phase-shifts. Figures 4A–4D correspond to Figs 1A–1D, and *black and white ovals* represent low and high intensity in *VA*, respectively. The gradient factors were projected in the plane determined by the frequency and slice axes, ie, in the coronal plane (*X-Z* plane specified in Fig. 3) for *A*, *B*, and *D*, and in the sagittal plane (*Y-Z* plane in Fig. 3) for *C*. On the basis of the measured angles between the *VA*s and each axis on MR angiograms (data not shown) projected in the sagittal and coronal plane, each figure was depicted. The direction of the gradient factors, which varies with imaging parameters such as slice thickness, field of view, or matrix size even when the same sequence is used, was calculated under the parameter setting employed.

A, Routine T1-weighted sequence: coronal orientation illustrating effective gradient factor. The direction of gradient factor has a nearly perpendicular orientation in relation to right *VA*.

B, T1-weighted sequence with polarity reversal of the frequency-encoding gradient: coronal orientation showing effective gradient factor. The inversion of polarity results in a rotation of gradient factor about the slice axis. In this case, the direction of gradient factor is nearly perpendicular in relation to left *VA*.

C, T1-weighted sequence with swapped phase and frequency orientation: sagittal orientation showing effective gradient factor. Gradient factor is nearly perpendicular to *VA* on both sides.

D, T1-weighted sequence with gradient moment nulling: no net effective gradient factor.

of the frequency- and phase-encoding axes, or with the use of motion-compensating gradients, the corresponding gradient factor was nearly perpendicular to the flow directions in both *VA*s (Fig. 4C) or nonexistent (Fig. 4D). Therefore, because of the insensitivity to motion-induced phase-shift effects for both cases, the vertebral arteries were symmetrically represented as high intensity (Figs. 1C and 1D).

For the first echo of the dual-echo sequence, the gradient waveform was identical to that used for the T1-weighted spin-echo sequence illustrated in Figure 1A, indicating that both had the same sensitivity to motion-induced phase-shift effects. This explains why a similar appearance with high intensity visible in the right *VA* was seen between the proton density-weighted image (Fig. 2A) and the T1-weighted image (Fig. 1A).

Because a long TE of 90 msec was used for the second echo, outflow signal loss would become dominant, thereby leading to the familiar flow void in both *VA*s despite the use of flow compensation (Fig. 2B). In contrast to spin-echo imaging, there is no refocusing 180° radio frequency pulse in gradient-echo imaging. Therefore, on gradient-echo images, outflow signal loss does not occur, but any unsaturated spins moving into the imaging plane yield an increased signal at almost all flow rates when a single slice is obtained. Because of the combination of this feature of gradient-echo imaging with the use of flow compensation, the gradient-echo image (Fig. 2C) showed extremely high intensity in both *VA*s. Anatomic differences between a pair of vertebral arteries, such as in caliber size, can be a cause of asymmetric appearance on MR images. However, the MR angiogram (Fig. 2D) demonstrated the symmetric appearance of the vertebrobasilar system for this subject, indicating that the variable appearances of the vertebral arteries on the MR images we have described has no relevance to subject-dependent factors.

The default directions of the frequency- and phase-encoding axes on the Siemens MR unit, although exchangeable, are horizontal and vertical, respectively. In this condition, pairs of right and left intracranial vessels other than vertebral arteries, even with similar flow between them, may demonstrate asymmetric appearances because of the reason described above (Fig. 5). Some other manufacturers (eg, General Electric) adopt the alternative default allocation of these axes in axial imaging of the head, ie, the horizontal phase- and vertical frequency-encoding directions. This choice of allocation may be preferable for demonstrating the same intensity for a pair of intracranial vessels with similar flow, since the sensitivity to motion-induced phase-shift effects has no preferred orientation in the horizontal direction. The use of motion-compensating gradients is also effective for this purpose, but may lead to resulting penalties such as a longer time to echo and/or a decrease in the signal-to-noise ratio due to an increase in the receiver band width.

In summary, the interaction between the slice-selection and frequency-encoding gradients leads to variable phase shifts of obliquely traversing spins through the imaging plane, depending on the angle between the direction of flow and that of the effective vector sum of these gradients. The asymmetric appearances of intracranial vessels in routine spin-echo axial imaging of the head we have described are a result of the angle dependence of motion-induced phase shifts. This phenomenon may be encountered in MR images of any region of the body (13). An awareness of this artifactual phenomenon that depends on MR imaging-related factors, including the orientation of the imaging plane and the frequency- and phase-encoding axes, is important in order to avoid misinterpreting these findings as pathologic conditions such as stenosis/occlusion, dissection, or slow flow.

Appendix

While the general expression for the additional phase accumulated because of motion, ϕ, including the effects of higher order motion like acceleration, is described elsewhere (14–16), for spins with a constant velocity of $\mathbb{V} = (v_x, v_y, v_z)$, ϕ is expressed as a simpler form of

$$\begin{aligned}\phi &= \mathbb{V} \cdot \mathbb{GF} \\ &= v_x GF_x + v_y GF_y + v_z GF_z,\end{aligned} \qquad \text{(A)}$$

where "·" denotes the dot product of the two vectors, and $\mathbb{GF} = (GF_x, GF_y, GF_z)$ is the gradient factor depending

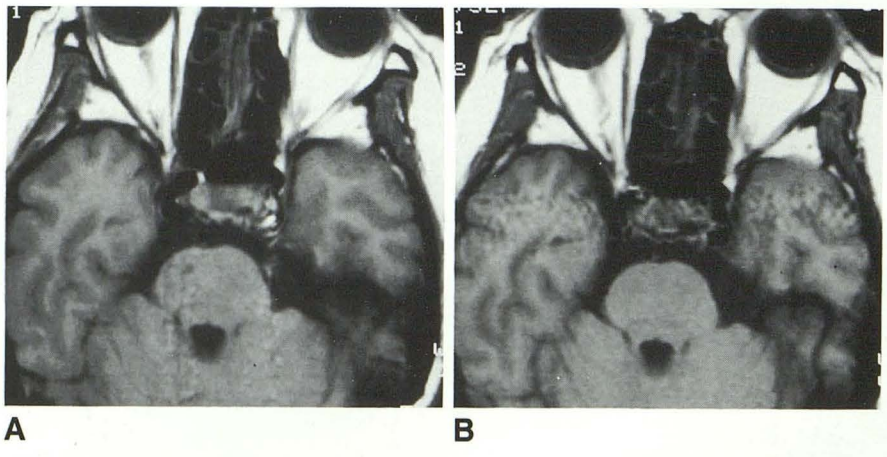

Fig. 5. T1-weighted spin-echo axial images through cavernous portion of internal carotid artery (ICA).

A, With the default allocation of the horizontal frequency and vertical phase axes, normal flow void is seen in right ICA; however, iso to hyperintense intravascular signal is recognized in left ICA. Note motion artifacts originating from ICA in the vertical phase-encoding direction.

B, With the exchange of the frequency and phase axes, normal flow void is vizualized in ICA on both sides. Note motion artifacts originating from ICA in the horizontal phase-encoding direction.

only on the set of imaging gradients, $\mathbb{G}$, used to obtain spatial information in the x-, y-, and z-axes. Equation A indicates that the net phase shift because of motion, ϕ, is a sum of the motion-induced phase shift, v_iGF_i in each direction, where suffix "i" corresponds to the x, y, or z axis. Since the dot product of two vectors, $\mathbb{A}$ and $\mathbb{B}$, is equivalent to $|\mathbb{A}|\ |\mathbb{B}|\cos\theta$, where θ is the angle between them, Equation A implies the dependence of the net motion-induced phase shift on the angle between the direction of flow and that of the gradient factor.

The explicit form of GF_i for single spin-echo pulse sequence is given by

$$GF_i = -\gamma \int_0^{TE/2} G_i dt + \gamma \int_{TE/2}^{TE} G_i dt, \qquad (B)$$

where γ is the gyromagnetic ratio. The phase-encoding directional component of $\mathbb{GF}$, GF_{phase} is usually small compared to those in the other directions and is variable because phase-encoding gradients change with each phase-encoding step. Even for the maximum phase-encoding gradient, GF_{phase} was only 33% of the frequency-encoding directional component of $\mathbb{GF}$ calculated for the single spin-echo pulse sequence without flow compensation. In the discussion, the contribution from this direction, therefore, was disregarded.

References

1. Alvarez O, Edwards JH, Hyman RA. MR recognition of internal carotid artery occlusion. *AJNR* 1986;7:359–360
2. Katz BH, Quencer RM, Kaplan JO, Hinks RS, Post MJ. MR imaging of intracranial carotid occlusion. *AJNR* 1989;10:345–350
3. Heinz ER, Yeates AE, Djang WT. Significant extracranial carotid stenosis: detection on routine cerebral MR images. *Radiology* 1989;170:843–848
4. Goldberg HI, Grossman RI, Gomori JM, et al. Cervical internal carotid artery dissecting hemorrhage: diagnosis using MR. *Radiology* 1986;158:157–161
5. McMurdo SK, Brant-Zawadzki M, Bradley WG, et al. Dural sinus thrombosis: study using intermediate field strength MR imaging. *Radiology* 1986;161:83–86
6. Pattany PM, Phillips JJ, Chiu LC, et al. Motion artifact suppression technique (MAST) for MR imaging. *J Comput Assist Tomogr* 1987;11:369–377
7. Whittemore AR, Bradley WG, Jinkins JR, et al. Comparison of cocurrent and countercurrent flow-related enhancement in MR imaging. *Radiology* 1989;170:265–271
8. Axel L. Blood flow effects in magnetic resonance imaging. *AJR* 1984;143:1157–1166
9. Bradley WG, Waluch V, Lai KS, Fernandez EJ, Spalter C. The appearance of rapidly flowing blood on magnetic resonance images. *AJR* 1984;143:1167–1174.
10. Valk PE, Hale JD, Crooks LE, et al. MRI of blood flow: correlation of image appearance with spin-echo phase shift and signal intensity. *AJR* 1986;146:931–939
11. Von Schulthess GK, Higgins CB. Blood flow imaging with MR: spin-phase phenomenon. *Radiology* 1985;157:687–695
12. Larson TC, Kelly WM, Ehman RL, Wehrli FW. Spatial misregistration of vascular flow during MR imaging of the CNS: cause and clinical significance. *AJNR* 1990;11:1041–1048
13. Mayo J, McVeigh ER, Hoffman N, Poon PY, Henkelman RM. Disappearing illiac vessels: an MR phase cancellation phenomenon. *Radiology* 1987;164:555–557
14. Wendt RE, Murphy PH, Ford JJ, Bryan RN, Burdine JA. Phase alterations of spin echoes by motion along magnetic field gradients. *Magn Reson Med* 1985;2:527–533
15. Katz J, Peshock RM, McNamee P, Schaefer S, Malloy CR, Parkey RW. Analysis of spin-echo rephasing with pulsatile flow in 2D FT magnetic resonance imaging. *Magn Reson Med* 1987;4:307–322
16. Fujita N, Harada K, Murakami T, Akai Y, Kozuka T. Effects of velocity profile of to-and-fro pulsatile flow on magnetic resonance signal intensity. *Magn Reson Med* 1990;15:275–286